

Scaling in the crossover from random to correlated growth

F. D. A. Aarão Reis

Instituto de Física, Universidade Federal Fluminense, Avenida Litorânea s/n, 24210-340 Niterói RJ, Brazil

(Received 24 August 2005; published 22 February 2006)

In systems where deposition rates are high compared to diffusion, desorption, and other mechanisms that generate correlations, a crossover from random to correlated growth of surface roughness is expected at a characteristic time t_0 . This crossover is analyzed in lattice models via scaling arguments, with support from simulation results presented here and in other works. We argue that the amplitudes of the saturation roughness and of the saturation time t_\times scale as $t_0^{1/2}$ and t_0 , respectively. For models with lateral aggregation, which typically are in the Kardar-Parisi-Zhang (KPZ) class, we show that $t_0 \sim p^{-1}$, where p is the probability of the correlated aggregation mechanism to take place. However, $t_0 \sim p^{-2}$ is obtained in solid-on-solid models with single-particle deposition attempts. This group includes models in various universality classes, with numerical examples being provided in the Edwards-Wilkinson (EW), KPZ, and Villain-Lai-Das Sarma (nonlinear molecular-beam epitaxy) classes. Most applications are for two-component models in which random deposition, with probability $1-p$, competes with a correlated aggregation process with probability p . However, our approach can be extended to other systems with the same crossover, such as the generalized restricted solid-on-solid model with maximum height difference S , for large S . Moreover, the scaling approach applies to all dimensions. In the particular case of one-dimensional KPZ processes with this crossover, we show that $t_0 \sim \nu^{-1}$ and $\nu \sim \lambda^{2/3}$, where ν and λ are the coefficients of the linear and nonlinear terms of the associated KPZ equations. The applicability of previous results to models in the EW and KPZ classes is discussed.

DOI: [10.1103/PhysRevE.73.021605](https://doi.org/10.1103/PhysRevE.73.021605)

PACS number(s): 81.15.Aa, 05.40.-a, 05.50.+q, 68.55.-a

I. INTRODUCTION

The large number of technological applications of thin films and multilayers motivates the study of continuous and atomistic models for the growth of those structures [1–3]. Their morphology is often the product of a competition between different growth dynamics; thus, theoretical models representing such features have received increasing attention in recent years. Some examples are the models with aggregation of different species of particles [4–6] or those mixing different microscopic aggregation rules for the same species [7–17].

In processes starting from a flat surface where the deposition rate is high compared to ad-particle diffusion coefficients, a random growth is initially observed, with negligible spatial correlations in the local thicknesses. Subsequently, diffusion, desorption, and other mechanisms introduce surface correlations, and consequently, a crossover from random to correlated growth is observed. The simplest quantitative characteristic of the film surface which reveals this crossover is the average roughness (or interface width), defined as the rms fluctuation of the height h around its average position \bar{h} : $W(L, t) \equiv [\langle (h - \bar{h})^2 \rangle]^{1/2}$. The aim of this work is to study scaling relations for the surface roughness in lattice models which present this crossover.

In a random, uncorrelated growth, the roughness increases as

$$W_r \sim t^{1/2}. \quad (1)$$

On the other hand, in correlated growth processes, it is expected to obey the Family-Vicsek scaling relation [18]

$$W(L, t) \approx AL^\alpha f\left(\frac{t}{t_\times}\right), \quad (2)$$

where L is the system size, α is the roughness exponent, A is a model-dependent constant, f is a scaling function such that $f \sim 1$ in the regime of roughness saturation ($t \rightarrow \infty$), and t_\times is the characteristic time of crossover to saturation. t_\times scales with the system size as

$$t_\times \approx BL^z, \quad (3)$$

where z is the dynamic exponent and B is another model-dependent amplitude. For $t \ll t_\times$ (after a possible crossover to correlated growth), the roughness scales as

$$W \approx Ct^\beta, \quad (4)$$

where C is constant and $\beta = \alpha/z$ is the growth exponent. In this growth regime, $f(x) \sim x^\beta$ in Eq. (2).

Figure 1 illustrates the time evolution of the surface roughness in systems which present a crossover from random to correlated growth at a characteristic time t_0 (this time is also called $t_{\times 1}$ and τ_h by other authors [11,16,19]). For t

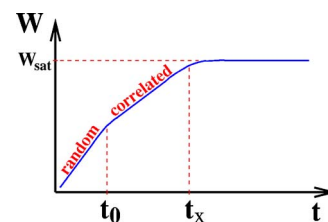


FIG. 1. (Color online) Typical time behavior of the interface width W in a system with crossover from random to correlated growth at time t_0 and crossover to saturation at time t_\times .

$< t_0$, W increases as Eq. (1), and the reduced slope in the subsequent regime ($t_0 \ll t \ll t_\times$) is a signature of the smoothing effect of correlations. In systems where a correlation mechanism and a random growth mechanism are simultaneously present, a different balance of these mechanisms changes the crossover time t_0 , which affects the amplitudes A , B , and C [Eqs. (2)–(4)].

This was observed by Horowitz *et al.* [7,10,11], who studied numerically two-component models in which different rules for the aggregation of the same species are chosen, with complementary probabilities (they are simply called competitive models by several authors [7,10–14,16]). The first component of those models, with probability $1-p$, was random deposition (RD): particles attach to the top of the column of incidence independently of the neighboring heights. In their first competitive model (called the RD-BD model), the second component was ballistic deposition (BD) [20], with probability p . In their second competitive model (called RD-RDSR), the correlated component was random deposition with surface relaxation (RDSR) [21]. As expected from the absence of correlations in RD, the universal scaling exponents α , β , and z of the competitive models are those of the universality class of the correlated component [17]. However, the scaling amplitudes are affected and scale with p as [7,10,11]

$$A \sim p^{-\delta}, \quad (5)$$

$$B \sim p^{-\gamma}, \quad (6)$$

and

$$C \sim p^{-\gamma}. \quad (7)$$

For the RD-BD model, $\delta=1/2$ and $\gamma=1$ were obtained in all substrate dimensions d [10,11]. For the RD-RDSR model, $\delta=1$ and $\gamma=2$ were obtained [7,11]. In both competitive models, the exponent γ depended on d .

In a recent work, Braunstein and Lam [16] explained the differences between those systems through scaling arguments which account for the average height increase and fluctuations during the time interval between two correlated deposition events. Previously, the equation representing the RD-RDSR model in the continuum limit was also derived [14]. Since those works analyzed particular models in the Edwards-Wilkinson (EW) [22] and in the Kardar-Parisi-Zhang (KPZ) [23] classes, the picture that emerged from those results was that the exponents δ and γ are related to the universality class of the dominant process: $\delta=1/2$ and $\gamma=1$ in the crossover to KPZ, $\delta=1$ and $\gamma=2$ in the crossover to EW. The dominant behavior of another competitive model in Ref. [16] was not trivial to infer, but the crossover exponents to KPZ and EW were the same. However, recent numerical work by Kolakowska *et al.* [15,17] shows that $\delta=1$ and $\gamma=2$ is also found in two-component models in the KPZ class. Thus, a complete theoretical explanation of the values of these crossover exponents is still lacking.

Here we will present a scaling approach which provides such an explanation through a connection of roughness amplitudes, crossover times, and the microscopic rules of the lattice models. It can be applied to all spatial dimensions and

to all types of correlated growth and agrees with our numerical results for models in three different universality classes and with numerical results from other authors works [10,11,19].

We will argue that $A \sim t_0^{1/2}$ and $B \sim t_0$ in the models with random to correlated crossover, so that t_0 acts as a time dilatation factor. The relations between t_0 and the parameters of the discrete models are subsequently obtained by scaling arguments, partially rephrasing those of Braunstein and Lam [16]. These arguments lead to a separation of the lattice models in two groups: the first one includes solid-on-solid models with single-particle deposition attempts, for which $\delta=1$ and $\gamma=2$, and the second one includes models with lateral aggregation, for which $\delta=1/2$ and $\gamma=1$. This classification is independent of the universality class of the correlated process; consequently, KPZ processes may be found in both groups—i.e., with different crossover exponents. Moreover, our theoretical approach comprises not only two-component models involving RD, but can be extended to other models with the same crossover. One example is the generalized restricted solid-on-solid (RSOS) model, with maximum height difference S between neighbors [19], which presents that crossover for large S [with p replaced by S^{-1} in Eqs. (5)–(7)] and which will be studied numerically here.

The theoretical analysis is motivated in Sec. II, with the presentation of several discrete models showing the random to correlated crossover and the discussion of their simulation results. The scaling approach is presented in Sec. III, and in Sec. IV we summarize our conclusions.

II. LATTICE MODELS AND SIMULATION RESULTS

First we recall the models with crossover from random to correlated growth previously studied by other authors.

The first one is RD-BD [10]. In pure BD ($p=1$), the particle sticks at first contact with a nearest neighbor, as illustrated in Fig. 2(a), which leads to the formation of a porous deposit. Simulations of the RD-BD model gave $\delta \approx 1/2$ and $\gamma \approx 1$ in $d=1$, $d=2$, and $d=3$ [10,11], while γ depended on d . From the Family-Vicsek relation (2) and the p scaling for the amplitudes A , B , and C [Eqs. (5)–(7)], Horowitz and Albano proposed that

$$\beta\gamma - \delta + \gamma = 0 \quad (8)$$

in any d , which agrees with their simulation results [10,11]. Here β is the growth exponent of the KPZ class.

The KPZ equation, which describes BD in the continuum limit, is

$$\frac{\partial h}{\partial t} = \nu \nabla^2 h + \frac{\lambda}{2} (\nabla h)^2 + \eta(\vec{x}, t), \quad (9)$$

where h is the height at the position \vec{x} in a d -dimensional substrate at time t , ν represents a surface tension, λ represents the excess velocity, and η is a Gaussian noise [2,23] with zero mean and covariance $\langle \eta(\vec{x}, t) \eta(\vec{x}', t') \rangle = D \delta^d(\vec{x} - \vec{x}') \delta(t - t')$. In $d=1$, the exact KPZ exponents are $\alpha=1/2$, $\beta=1/3$, and $z=3/2$, and in $d \geq 2$ approximate values are given in Refs. [24,25]. In models with a crossover from ran-

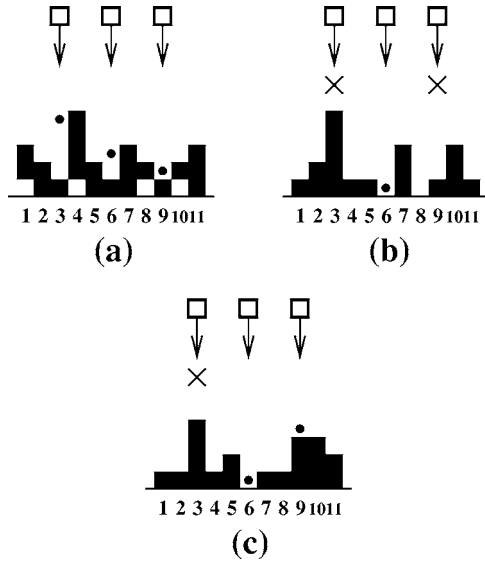


FIG. 2. Aggregation rules of lattice models in $d=1$, in which solid squares represent aggregated particles, open squares represent incident particles, with the column of incidence indicated by arrows, small bullets indicate the aggregation position of the incident particles, and crosses indicate rejected attempts of deposition. The rules of ballistic deposition are illustrated in (a). The conditions for RSOS aggregation (probability p) in the competitive model RD-RSOS are illustrated in (b). The generalized RSOS model with $S=3$ is illustrated in (c). Column labels are indicated below the substrate lines.

dom to KPZ growth, small values of ν and λ are expected in the corresponding KPZ equation.

The second model studied by those authors was RD-RDSR [7]. In pure RDSR ($p=1$), the incident particle diffuses to the column with minimum height in its nearest neighborhood [21]. RDSR is described by the EW equation, which corresponds to Eq. (9) with $\lambda=0$. In $d=1$, $d=2$, and $d=3$, the exponents $\delta=1$ and $y=2$ [11] were obtained for the RD-RDSR model, while the exponent γ also depended on d .

Other models involving competition with RD in $d=1$ were recently proposed in Refs. [15,17]. One example is a model whose correlated component allows aggregation of the incident particle only at surface minima [17]. It is in the KPZ class, but has $\delta \approx 1$ and $y \approx 2$.

In the following, we will present our numerical results for three models devised to broaden the investigation on the crossover exponents.

The first one is also a two-component model, involving RD with probability $1-p$. With probability p , the aggregation is possible only if the height of the column of incidence does not exceed the heights of any of its neighbors; otherwise, the aggregation attempt is rejected, as shown in Fig. 2(b). In other words, aggregation is possible only in valleys or plateaus. This model mimics a competition between RD and RSOS deposition; thus, we call it the RD-RSOS model. We refer to the correlated component as RSOS because it works against the formation of large local slopes, as illustrated in Fig. 2(b) (there, the attempts at columns 3 and 9 are rejected because one or more neighbors have smaller heights). In the pure RSOS model [26] ($p=1$), the above

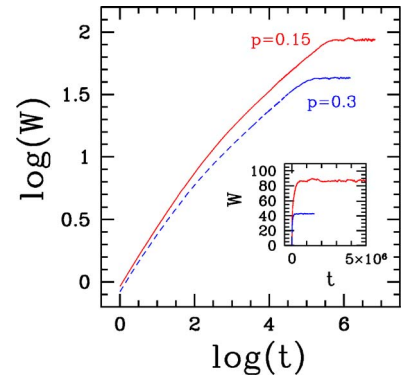


FIG. 3. (Color online) Time evolution of the roughness of the RD-RSOS model in lattices with $L=256$, for two different probabilities p . The inset shows a linear plot of the same quantities.

aggregation rule implies $\Delta h_{max}=1$ between neighboring columns.

The RD-RSOS model was simulated in one-dimensional lattices with $32 \leq L \leq 512$ for some values of p in the range $0.12 \leq p \leq 0.4$. Here 10^4 realizations were obtained for the smallest lattices and 10^3 for the largest ones. For the same values of p , the model was simulated in substrates with $L=8192$ during the random and the KPZ growth regimes.

In Fig. 3 we show the time evolution of the roughness for $p=0.15$ and $p=0.3$ in lattices with $L=256$. For both values of p , it is clear that the roughness behaves as in the sketch of Fig. 1. The saturation regimes are clearer in the linear plot of the inset, which shows that the saturation roughness approximately doubles when p is reduced from 0.3 to 0.15. Using Eqs. (2) and (5), this suggests $\delta \approx 1$. The parallel lines of the KPZ growth regimes illustrate the behavior described by Eqs. (4) and (7), with the amplitude C increasing as p decreases.

In order to obtain reliable estimates of the crossover exponents, we analyzed the effects of finite L , t , and p , taking the limits $L \rightarrow \infty$, $t \rightarrow \infty$, and $p \rightarrow 0$ when appropriate. This procedure was proved to be essential to avoid erroneous conclusions on the class of several growth models (see, e.g., the analysis of BD in [27]). For a fixed value of p , our first step is to extrapolate W_{sat}/L^α to $L \rightarrow \infty$, using $\alpha=1/2$, as illustrated in Fig. 4(a) for $p=0.25$. From Eq. (2), the asymptotic value of that ratio is the amplitude $A(p)$ [$A \approx 3.18$ in Fig. 4(a)]. For each pair of subsequent probabilities p' and p'' , we define the effective exponents

$$\delta_p = \frac{\ln[A(p')/A(p'')]}{\ln(p''/p')}, \quad (10)$$

where p is an average probability:

$$p \equiv \sqrt{p'p''}. \quad (11)$$

As p' and p'' decrease, $p \rightarrow 0$ and $\delta_p \rightarrow \delta$. In Fig. 4(b) we show δ_p versus p^2 , which suggests $\delta \approx 1$.

The first step to estimate γ is to extrapolate $W/t^{1/3}$ in the growth regime, using the data from lattices with $L=8192$. For fixed p , that ratio converges to $C(p)$ as $t \rightarrow \infty$ [Eq. (4)]. This is illustrated in Fig. 4(c) for $p=0.2$, where we obtain

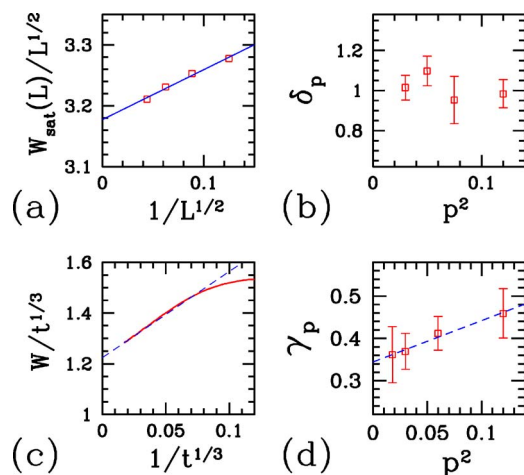


FIG. 4. (Color online) (a) Extrapolation of the ratio W_{sat}/L^α to $L \rightarrow \infty$, with $\alpha=1/2$, for the RD-RSOS model in $d=1$ with $p=0.25$ and $64 \leq L \leq 512$. (b) Effective exponents δ_p versus squared probability p^2 for the RD-RSOS model. (c) Extrapolation of the ratio W/t^β to $t \rightarrow \infty$, with $\beta=1/3$, for the RD-RSOS model in $d=1$ with $p=0.2$ and $L=8192$. (d) Effective exponents γ_p versus squared probability p^2 for the RD-RSOS model, with a least-squares fit of the data.

$C \approx 1.22$ (this extrapolation represents the long-time behavior in an infinitely large substrate). The effective exponents γ_p were calculated from $C(p)$ along the same lines of the calculation of δ_p in Eq. (10). They are shown in Fig. 4(d) as a function of p^2 , which suggests $\gamma \approx 1/3$ as $p \rightarrow 0$. The estimates of δ and γ and Eq. (8) give $y \approx 2$ for the RD-RSOS model.

Thus, although the RD-RSOS model is in the KPZ class, similarly to the RD-BD model, its crossover exponents δ and y are the same as the RD-RDSR model, which is in the EW class.

The second model analyzed here does not involve competition of aggregation rules. It is called the generalized RSOS model and was originally proposed in Refs. [26,28]. The incident particle can aggregate at a certain column only if the height differences between neighboring columns do not exceed an integer value S ; otherwise, the deposition attempt is rejected. The version with $S=3$ is illustrated in Fig. 2(c). For large S , with an initially flat substrate, random growth occurs until a significant fraction of neighboring columns has height difference S . Subsequently, KPZ growth is observed due to the rejection of deposition attempts.

The generalized RSOS model was studied numerically by Chien *et al.* [19], who obtained $t_0 \sim S^{2.06}$ for large S , in agreement with their scaling arguments, which give $t_0 \sim S^2$. However, the roughness amplitudes were not calculated there.

Here it was simulated until saturation in one-dimensional lattices with $32 \leq L \leq 512$ for several values of S in the range $4 \leq S \leq 32$. The number of realizations was 10^4 for the smallest lattices and 10^3 for the largest ones. We also simulated the model in $L=8192$ up to $t \gg t_x$, with 10^3 realizations for each S .

For any S , the height difference $\Delta h \equiv h_{i+1} - h_i$ of neighboring columns can assume $2S+1$ different values. However, deposition attempts are rejected only when Δh is $-S$ or $+S$,

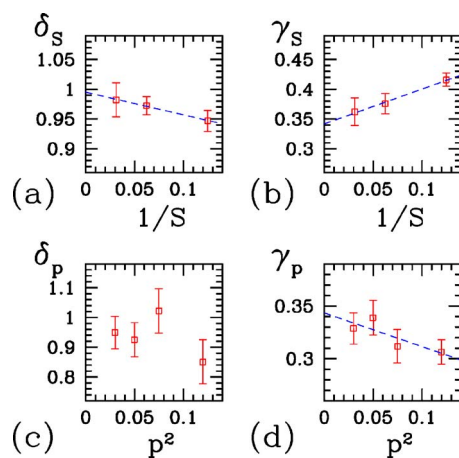


FIG. 5. (Color online) (a), (b) Effective exponents δ_S and γ_S versus $1/S$ for the generalized RSOS model. (c), (d) Effective exponents δ_p and γ_p versus squared probability p^2 for the RD-CRSOS model. The dashed lines in (a), (b), and (d) are least-squares fits of the data.

because those attempts would lead to height differences $-(S+1)$ and $S+1$. For large S , it is reasonable to assume that all values of Δh have nearly the same probability; thus, the probability of rejecting aggregation is of order $2/(2S+1) \approx S^{-1}$. Since aggregation rejection is the mechanism to spread correlations, S^{-1} plays the same role of p in the other competitive models. Thus we assume that

$$A(S) \sim S^\delta, \quad (12)$$

$$B(S) \sim S^y, \quad (13)$$

and

$$C(S) \sim S^\gamma \quad (14)$$

in the generalized RSOS model.

Estimates of the crossover exponents δ and γ were obtained along the same lines of the RD-RSOS model described above. First, for fixed S , the extrapolation of $W_{\text{sat}}/L^{1/2}$ provided estimates of the amplitude $A(S)$. Finite-size estimates of the exponent δ are given by

$$\delta_S = \frac{\ln[A(S)/A(S/2)]}{\ln 2}. \quad (15)$$

Their values are shown in Fig. 5(a) as a function of $1/S$, suggesting $\delta \approx 1$ asymptotically. Amplitudes $C(S)$ were obtained from the extrapolation of $W/t^{1/3}$ in the KPZ growth regime of large substrates, and effective exponents γ_S were defined analogously to Eq. (15). They are shown in Fig. 5(b) as a function of $1/S$, suggesting $\gamma \approx 1/3$ asymptotically. Those values also lead to $y \approx 2$.

The third model analyzed here is a two-component one which belongs to the class of the Villain–Lai–Das Sarma (VLDS) equation [29,30]. Again, RD has probability $1-p$. With probability p , aggregation is allowed only at valleys or plateaus, similarly to the RD-RSOS case. However, if aggregation is not possible at the column of incidence, then the incident particle migrates to the nearest column in which that

condition is satisfied and is irreversibly attached there. When $p=1$, we obtain the conserved restricted solid-on-solid (CRSOS) model of Kim *et al.* [31], where heights differences between neighboring columns do not exceed 1. However, with $p < 1$, differences of column heights larger than 1 appear due to the RD component. The competitive model will be called the RD-CRSOS model.

The original CRSOS model, as well as the RD-CRSOS model, is represented in the continuum limit by the VLDS equation (also called nonlinear molecular-beam epitaxy equation) [32,33]

$$\frac{\partial h}{\partial t} = \nu_4 \nabla^4 h + \lambda_4 \nabla^2 (\nabla h)^2 + \eta(\vec{x}, t), \quad (16)$$

where ν_4 and λ_4 are constants. The best known estimates of scaling exponents for the VLDS class were obtained from extensions of the CRSOS model; in $d=1$, they are $\alpha=0.93$ and $z=2.88$ [34], which gives $\beta=0.323$.

The RD-CRSOS model was simulated in one-dimensional lattices with the same values of p and L of the RD-RSOS model. In order to estimate the amplitudes A and C [Eqs. (2) and (4)], we used the above estimates of α and β . In Fig. 5(c) we show δ_p versus p^2 , which suggests $\delta \approx 1$, although the oscillations in the effective exponents do not allow a reliable extrapolation to $p \rightarrow 0$. In Fig. 5(d) we show γ_p versus p^2 , which suggests $\gamma \approx 1/3$. These values also lead to $y \approx 2$.

Thus, we have shown that a model in the VLDS class also has the crossover exponents of the previous solid-on-solid models in the EW and KPZ classes, differing only from the value of the RD-BD model.

III. SCALING THEORY FOR THE CROSSOVER FROM RANDOM TO CORRELATED GROWTH

First we discuss the universal features of this crossover in lattice models in any substrate dimension d , despite the illustrations being given in $d=1$ for simplicity (e.g., in Fig. 2). We consider here models without additional crossovers between different growth dynamics.

It is reasonable to assume that t_0 is the time in which the roughness of random growth [Eq. (1)] matches the growing roughness of the correlated process, Eq. (4) (see Fig. 1). This gives

$$C \sim t_0^{1/2-\beta}. \quad (17)$$

Now t_0 is the characteristic time for the onset of correlations among neighboring columns, which otherwise randomly grow. On the other hand, in a pure correlated model, the time $\delta t=1$ for deposition of one monolayer is enough to produce such correlations. Consequently, in models with the random to correlated crossover, we expect that all characteristic times are scaled by a factor t_0 . Since the amplitude of the saturation time t_\times is $B \sim 1$ for correlated models without additional crossover (BD, RDSR, RSOS, CRSOS, among others), we expect that

$$B \sim t_0 \quad (18)$$

when the crossover from random growth is present.

Now substituting the amplitude B from Eq. (18) in the Family-Vicsek relation (2) and considering that $f(x) \sim t^\beta$ in the growth regime ($t_0 \ll t \ll t_\times$), we obtain $W \sim (A/t_0^\beta)t^\beta$. Comparison with Eqs. (4) and (17) immediately leads to

$$A \sim t_0^{1/2}. \quad (19)$$

However, this relation may be obtained from different but consistent arguments, as follows. During time t_0 the neighboring columns randomly grow; thus, the local roughness W_l is of the order of the RD roughness $t_0^{1/2}$. W_l represents height fluctuations within narrow windows, whose sizes are of the order of one lattice unit, in a large lattice and at times long enough for significant correlations to appear inside those windows. On the other hand, when the global roughness W attains saturation, the whole system is also highly correlated. Thus, if the total system size is $L \sim 1$ (i.e., system size is small but not equal to 1), this system is a narrow window, and we expect $W_{sat} \sim W_l$. Since $W_{sat} \approx A$ in this case [Eq. (2) with $L=1$], we obtain Eq. (19). Certainly this argument does not apply to systems with anomalous scaling, where local and global roughness have different scaling properties, but that is not the case of the lattice models analyzed here or in related works.

Now we consider the particular properties of the lattice models, focusing on their small length-scale features. Our arguments are similar to those of Braustein and Lam [16] for the RD-BD and RD-RDSR models, but here we will emphasize the independence of the results of the universality class of the process. In all cases, correlated growth attempts have probability p , while uncorrelated growth takes place with probability $1-p$. Thus, in a given column, the mean time interval between two successive depositions that build up the correlations along the substrate is $\tau=1/p$.

Since BD involves lateral aggregation, a single deposition attempt following this model rules introduces height correlations between that column and the neighboring ones. This is illustrated by the deposition in column 3 of Fig. 2(a): the large height difference from column 4 is immediately suppressed by lateral aggregation. Consequently, in the RD-BD model, correlations between neighboring columns are built up within an average time interval τ . Consequently, we expect $t_0 \sim \tau$ in any spatial dimension. Using Eqs. (5), (6), (18), and (19), we obtain the exponents $\delta=1/2$ and $y=1$ for the RD-BD model, while Eqs. (7) and (17) provide exponents γ dependent on β and, consequently, dependent on the substrate dimension.

Now we consider the RD-RSOS model as a typical example of solid-on-solid model. In this case, a single RSOS attempt is not sufficient to balance the random growth of neighboring columns. For instance, consider the aggregation rejection in column 3 of Fig. 2(b): within the time interval τ , a single particle is expected to be deposited at columns 2 and 4, but these events do not suppress the large height difference from column 3. Thus, within a time interval of order τ , significant local correlations are not generated. Instead, in order for the rejection mechanism to balance the random growth locally, it is necessary that the number of rejected attempts at a given column be of the same order as the height difference between the neighbors. While the number of RSOS attempts

at a given column during time t increases as tp , the local height difference in random growth increases as $t^{1/2}$. Matching these values we obtain the crossover time $t_0 \sim p^{-2}$ for the RD-RSOS model. This result gives $\delta=1$ and $y=2$ in all dimensions. The exponent γ depends on the substrate dimension due to its dependence on the scaling exponent β [Eqs. (7) and (17)].

The same arguments apply to the crossover from random to EW scaling observed in the RD-RDSR model [7,11], since a single diffusion event to a lower height does not suppress a large height difference immediately. In the RD-CRSOS model, there is a combination of rejection of aggregation at high columns and diffusion to plateaus or valleys, but this combination also does not introduce significant height correlations immediately. Consequently, $t_0 \sim p^{-2}$ for these models, which lead to $\delta=1$ and $y=2$.

The features of the generalized RSOS model are explained by extending the arguments of Ref. [19]. Chien *et al.* [19] argued that KPZ growth takes place when the randomly growing roughness [Eq. (1)] is of order S , which gives $t_0 \sim S^2$. This is the same form of the previous solid-on-solid models, with S interpreted as a reciprocal probability of rejecting the aggregation. Thus, $\delta=1$ and $y=2$ for the generalized RSOS model.

All the above results are in full agreement with the simulation data shown in Sec. II. Although our simulation results (Sec. II) were limited to one-dimensional systems, Horowitz and Albano [11] presented simulation results for the RD-BD and RD-RDSR models in $d=1$, $d=2$, and $d=3$, and in all cases they agree with our predictions. In fact, no reference to a particular system dimension was done in the above arguments. Instead, they were only based on random growth properties [Eq. (1)], the Family-Vicsek relation [Eq. (2)], and the hypothesis of the existence of a crossover from random to correlated growth.

Our analysis clearly separated solid-on-solid models with single-particle aggregation attempts and models with lateral aggregation. Other limited-mobility growth models may be classified in one of these two groups by inspection of the microscopic aggregation rules of the correlated process. Since the exponents $\delta=1/2$ and $y=1$ are found in models with some type of lateral growth and, consequently, excess velocity, they are typical of models in the KPZ class. However, models in $\delta=1$ and $y=2$ may be found in any universality class of interface growth, including KPZ. Moreover, although most systems previously studied are two-component models, application to the generalized RSOS model shows that the crossover exponents and the above scaling approach may be extended to other systems presenting crossover from random to correlated growth.

Now we consider the particular case of KPZ systems in $d=1$, where relations between scaling amplitudes and the coefficients of the growth equation are known [35]:

$$A \sim \nu^{-1/2}, \quad (20)$$

$$B \sim \nu^{1/2} |\lambda|^{-1}, \quad (21)$$

and

$$C \sim \nu^{-2/3} |\lambda|^{1/3}. \quad (22)$$

In systems with a crossover from random to correlated growth, λ and ν may be arbitrarily small (but nonzero), while the noise amplitude D is finite; thus, the dependence on D is omitted in Eqs. (20)–(22). From Eqs. (19) and (20), we obtain

$$t_0 \sim \nu^{-1}, \quad (23)$$

and using Eqs. (18) and (21) we obtain

$$|\lambda| \sim \nu^{3/2} \quad (24)$$

in the crossover region of small ν and small $|\lambda|$.

These relations may also be obtained from the condition that the random-KPZ crossover takes place at the same time of the EW-KPZ crossover, $t_c \sim (C_{EW}/C_{KPZ})^{12} \sim \nu^5 \lambda^{-4}$ [13,36–38]. In other words, after leaving the random growth regime, those systems do not show an additional crossover from EW to KPZ because the linear and nonlinear effects simultaneously turn up.

Equations (23) and (24) provide relations between ν , $|\lambda|$, and the model parameter p or S . $\nu \sim p$ and $|\lambda| \sim p^{3/2}$ are obtained as particular relations for the RD-BD growth, but cannot be viewed as universal relations for the random to KPZ crossover in $d=1$. It contrasts to what could be naively believed from some works on competitive models with random to correlated crossover [10,11,16]. Instead, a large variety of KPZ processes, such as the RD-RSOS and generalized RSOS models, follow the relations $\nu \sim p^2$ and $|\lambda| \sim p^3$ in the crossover region in $d=1$. At this point, it is important to recall that previous numerical work on the RD-BD model did not calculate ν and λ directly from the growth velocities and interface shapes [10,11]. Instead, their relations with probability p were obtained from the scaling relations (20)–(22), similar to what was done in other competitive models [13] and in the present work.

IV. CONCLUSION

We studied limited-mobility growth models with crossover from random to correlated growth. Universal relations between the crossover time t_0 and the amplitudes of saturation roughness and saturation time were obtained from random deposition properties and Family-Vicsek scaling, for any spatial dimension. The lattice models with that crossover can be separated in two groups: the first one with lateral aggregation, such as ballistic deposition, in which correlations spread faster, and the second one of the solid-on-solid models with single-particle aggregation attempts, which require much longer times for the correlated aggregation to balance the random growth. While $t_0 \sim p$ in the first group, where p is the small probability of the correlated mechanism to work, in the second class we showed that $t_0 \sim p^2$. These relations are independent of the universality class of the process: although the first group is expected to include only KPZ processes, due to the presence of lateral growth, several KPZ models are also found in the second group. All these features are confirmed by simulations of lattice models in three different universality classes and different

substrate dimensions, partly obtained from other authors work. In $d=1$, relations between the probability p and the coefficients of the KPZ equation can be obtained for both groups of models.

Many natural and artificial processes involve the competition of different growth dynamics, and their analysis may

eventually be improved by extensions of our scaling arguments. In the case of KPZ scaling, although the connection between scaling amplitudes and the coefficients of the continuous equation is not trivial in $d > 1$, the numerical calculation of ν and λ may help the search for those relations, at least in the small- ν , small- λ limit.

-
- [1] *Frontiers in Surface and Interface Science*, edited by Charles B. Duke and E. Ward Plummer (Elsevier, Amsterdam, 2002).
- [2] A.-L. Barabási and H. E. Stanley, *Fractal Concepts in Surface Growth* (Cambridge University Press, New York, 1995).
- [3] J. Krug, *Adv. Phys.* **46**, 139 (1997).
- [4] W. Wang and H. A. Cerdeira, *Phys. Rev. E* **47**, 3357 (1993); H. F. El-Nashar and H. A. Cerdeira, *ibid.* **61**, 6149 (2000).
- [5] F. D. A. Aarão Reis, *Phys. Rev. E* **66**, 027101 (2002); **68**, 041602 (2003).
- [6] M. Kotrla, J. Krug, and P. Smilauer, *Phys. Rev. B* **62**, 2889 (2000).
- [7] C. M. Horowitz, R. A. Monetti, and E. V. Albano, *Phys. Rev. E* **63**, 066132 (2001).
- [8] Y. Shapir, S. Raychaudhuri, D. G. Foster, and J. Jorne, *Phys. Rev. Lett.* **84**, 3029 (2000).
- [9] Y. P. Pellegrini and R. Jullien, *Phys. Rev. Lett.* **64**, 1745 (1990); *Phys. Rev. A* **43**, 920 (1991).
- [10] C. M. Horowitz and E. V. Albano, *J. Phys. A* **34**, 357 (2001).
- [11] C. M. Horowitz and E. V. Albano, *Eur. Phys. J. B* **31**, 563 (2003).
- [12] T. J. da Silva and J. G. Moreira, *Phys. Rev. E* **63**, 041601 (2001).
- [13] A. Chame and F. D. A. Aarão Reis, *Phys. Rev. E* **66**, 051104 (2002).
- [14] D. Muraca, L. A. Braunstein, and R. C. Buceta, *Phys. Rev. E* **69**, 065103(R) (2004).
- [15] A. Kolakowska, M. A. Novotny, and P. S. Verma, *Phys. Rev. E* **70**, 051602 (2004).
- [16] L. A. Braunstein and C.-H. Lam, *Phys. Rev. E* **72**, 026128 (2005).
- [17] A. Kolakowska, M. A. Novotny, and P. S. Verma, e-print cond-mat/0509668.
- [18] F. Family and T. Vicsek, *J. Phys. A* **18**, L75 (1985).
- [19] C.-C. Chien, N.-N. Pang, and W.-J. Tzeng, *Phys. Rev. E* **70**, 021602 (2004).
- [20] M. J. Vold, *J. Colloid Sci.* **14**, 168 (1959); **63**, 1608 (1959).
- [21] F. Family, *J. Phys. A* **19**, L441 (1986).
- [22] S. F. Edwards and D. R. Wilkinson, *Proc. R. Soc. London, Ser. A* **381**, 17 (1982).
- [23] M. Kardar, G. Parisi, and Y.-C. Zhang, *Phys. Rev. Lett.* **56**, 889 (1986).
- [24] E. Marinari, A. Pagnani, and G. Parisi, *J. Phys. A* **33**, 8181 (2000).
- [25] F. D. A. Aarão Reis, *Phys. Rev. E* **69**, 021610 (2004).
- [26] J. M. Kim and J. M. Kosterlitz, *Phys. Rev. Lett.* **62**, 2289 (1989).
- [27] F. D. A. Aarão Reis, *Phys. Rev. E* **63**, 056116 (2001); *Physica A* (to be published).
- [28] J. M. Kim, J. M. Kosterlitz, and T. Ala-Nissila, *J. Phys. A* **24**, 5569 (1991).
- [29] J. Villain, *J. Phys. I* **1**, 19 (1991).
- [30] Z.-W. Lai and S. Das Sarma, *Phys. Rev. Lett.* **66**, 2348 (1991).
- [31] Y. Kim, D. K. Park, and J. M. Kim, *J. Phys. A* **27**, L533 (1994).
- [32] Z.-F. Huang and B.-L. Gu, *Phys. Rev. E* **57**, 4480 (1998).
- [33] S.-C. Park, D. Kim, and J.-M. Park, *Phys. Rev. E* **65**, 015102(R) (2002).
- [34] F. D. A. Aarão Reis, *Phys. Rev. E* **70**, 031607 (2004).
- [35] J. G. Amar and F. Family, *Phys. Rev. A* **45**, R3373 (1992).
- [36] T. Nattermann and L.-H. Tang, *Phys. Rev. A* **45**, 7156 (1992).
- [37] B. Grossmann, H. Guo, and M. Grant, *Phys. Rev. A* **43**, 1727 (1991).
- [38] B. M. Forrest and R. Toral, *J. Stat. Phys.* **70**, 703 (1993).